Zeta Potential of Microbubbles in Aqueous Solutions: Electrical Properties of the Gas-Water

DATASET · OCTOBER 2005

CITATIONS
7

READS
198

1 AUTHOR:

Masayoshi Takahashi
National Institute of Advanced Industrial Sci…
32 PUBLICATIONS **644** CITATIONS

SEE PROFILE

ζ Potential of Microbubbles in Aqueous Solutions: Electrical Properties of the Gas−Water Interface

Masayoshi Takahashi*

National Institute of Advanced Industrial Science and Technology (AIST), 16-1 Onogawa, Tsukuba, Ibaraki 305-8569, Japan

Received: December 1, 2004; In Final Form: September 4, 2005

Microbubbles are very fine bubbles and appropriate for the investigation of the gas−water interface electrical charge, because of their long stagnation, due to slow buoyancy, in the electrophoresis cell observation area. This study investigated the ζ potential of microbubbles in aqueous solutions and revealed that the bubbles were negatively charged under a wide range of pH conditions. The potential was positive under strong acidic conditions, and the inorganic electrolytes decrease the potential by increasing the amount of counterions within the slipping plane. OH^- and H^+ are crucial factors for the charging mechanism of the gas−water interface, while other anions and cations have secondary effects on the ζ potential, because counterions are attracted by the interface charge. The addition of a small amount of propanol and butanol provided significant information for considering the mechanism of the gas−water interface charge. Even though these alcohols did not have any electrical charge, they had a strong effect on the gas−water interface charge and dispersed the ζ potential of the microbubbles in the aqueous solution. These alcohols tended to adsorb to the interface and affect the hydrogen-bonding network at the interface, so that it was concluded that the gas−water interface electrical charge must be related to the difference of the construction of the hydrogen-bonding network between the bulk water and the gas−water interface.

Introduction

The electrical properties of gas bubbles are important in determining the interaction of bubbles in coalescence and the way bubbles interact with other materials, such as solid particles and oil droplets, to provide a basis for technical application in many fields, such as foam fractionation, food processing, and purification processes.[1−4] Most of the previous studies on the surface charge of bubbles have been conducted with electrophoresis methods.[5−16] These studies have demonstrated that the bubbles in distilled water are negatively charged and that simple inorganic electrolytes change the magnitude of the bubble charge without altering the sign of the charge, on the condition that any precipitates are not adsorbed at the gas−water interface. However, it has been very difficult to conduct systematic research to clarify the charging mechanism by electrophoretic methods, because the motion imparted by the electric field is difficult to distinguish in the presence of a gravitational field. Recently, new technologies have been established to produce very fine bubbles with a diameter less than 50 μm in aqueous fluids, permitting the precise evaluation of the electric properties of the gas−water interface without any complicated technique in the electrophoresis method. This study has clarified the effects of additional electrolytes and alcohols on the bubble charge and has approached a mechanism of gas−water interface electrical property.

Microbubble

One of the most significant characters of a microbubble less than 50 μm in diameter is the decrease in size and subsequent collapse under water, because of long stagnation and excellent gas dissolution ability. There are some conventional methods of producing bubbles in water such as supplying gas through small pores or shearing a gas body with rotating blades. It is difficult to produce microbubbles without the addition of any electrolytes or surfactants into the water, because of the strong surface tension of water. Recently, several methods have been invented to generate very fine gas bubbles in aqueous solutions, and Figure 1 shows a microbubble aerator used in this study.

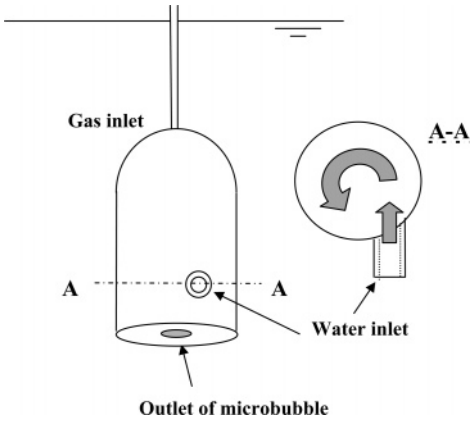

Figure 1. Microbubble aerator. Water was introduced through the water inlet using a water pump and spiraled up along the wall. The centrifugal force, caused by the circulating flow, automatically introduces a gas from the gas inlet, and the vortex of gas that formed along the center axis was strongly separated into fine bubbles at the outlet of the apparatus by the shearing force of the dispersed water.

Water introduced into the apparatus by a pump is spiraled up along the wall and down to the outlet along the center of the apparatus. The centrifugal force caused by the circulating flow automatically introduces a gas from the gas inlet, and a

* Phone: +81-29-861-8783. Fax: +81-29-861-8496. E-mail: m.taka@aist.go.jp.

10.1021/jp0445270 CCC: $30.25
Published on Web 10/29/2005

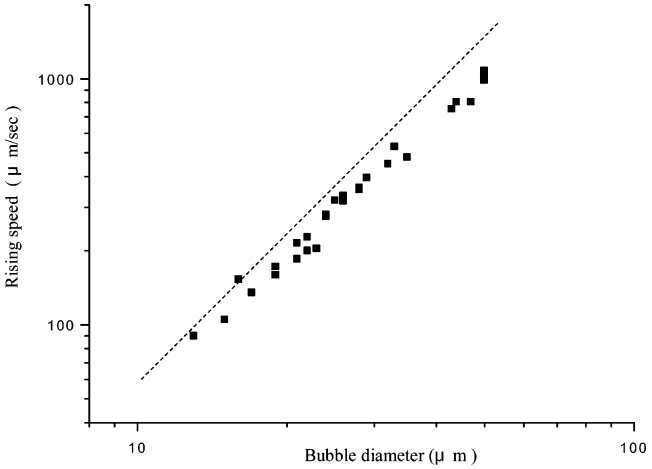

Figure 2. Rising speed of microbubbles in distilled water (the electric conductivity was less than 1.5 μS/cm). The speed was roughly described by the theoretical values of Stokes' law (the dashed line).

vortex of gas is formed along the center axis. The gas body is separated into fine bubbles at the outlet of the apparatus by the strong shearing force of the dispersed water and the circulation power.

The rising speed of the microbubble is a very important factor for the consideration of electrokinetic properties, and this was measured in a small transparent cell with a microscope system, described below, with magnification from ×200 to ×400 and imaging of 640 × 480 pixels at 30 frames/s. The estimated error for the measurement of the bubble diameter was less than 5%. The rising speed was evaluated by the distance each bubble moved over a period of greater than 1 s, using graphic data processing. Figure 2 shows the rising speed as a function of bubble diameter, and it has been demonstrated that the speed was roughly described by the theoretical values of Stokes' law.[17]

$$V = 1/18 \times gd^2/\nu$$

where V (m/s) is the rising velocity of the bubble, g (m/s^2) is the gravitational acceleration, d (m) is the diameter of the bubble, and ν (m^2/s) is the kinematic viscosity of water. The rising speed of 50 μm microbubbles is approximately 1 mm/s, and the long stagnation of microbubbles in the observation field of the electrophoresis cell enabled the evaluation of the electrical properties of the gas−water interface by measuring the ζ potential of microbubbles with a noncomplicated measuring system.

Method

Figure 3 shows a schematic diagram of the experimental setup for the study. The apparatus used for the measurements was of the microelectrophoresis type. The setup consisted of a water reservoir with a microbubble aerator, an electrophoresis cell, two electrodes and a constant voltage power source, water pumps, a microscope system with a magnification lens of ×75, and a computer. The electrophoresis cell was composed of quartz glass with stainless steel sides; the internal dimensions of the rectangular cell were 1.0 mm thick, 23.0 mm wide, and 75.0 mm long. The cell was positioned vertically, relative to the microscope objective. The electrodes consisted of silver axles and silver thin plates bent to a spiral shape with a 120 cm^2 contact area with the surrounding water. These electrodes were settled in stainless steel cells under an electrically isolated condition, and the cells were connected to the stainless steel sides of the electrophoresis cell with stainless steel pipes. An

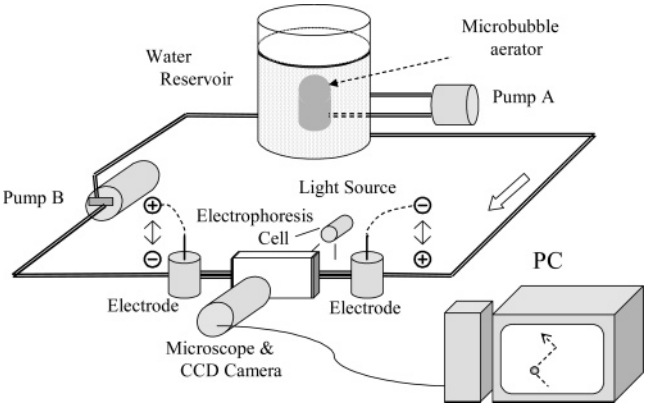

Figure 3. Experimental setup of the study. The microbubble aerator generated very fine bubbles in the water reservoir (approximately 10 L). The bubbles were introduced into an electrophoresis cell, and the movement of the microbubbles was analyzed under an electric field for the determinations of bubble diameter and ζ potential using a graphic data processing method.

electric voltage of 350 V was supplied to the electrodes using a constant voltage power source through a transfer switch which was used to change the direction of the electric potential drop in the electrophoresis cell. The real voltage difference between both ends of the electrophoresis cell was checked with a potentiometer. Microbubbles generated by the aerator in the water reservoir were introduced to the electrophoresis cell using water pump B and were observed using the microscope system. Light was scattered using thin white screens behind the cell, for clear observation of the spherical bubbles in the cell.

The experimental difficulty of studying electrophoretic mobility is related to the effect of electroosmotic flow in the cell. Electroosmosis is caused by the formation of an electric double layer at the surface of the cell wall which subsequently creates a movement of the aqueous solution. The electrophoresis related to the double layer at the gas−water surface creates a movement of bubbles in the aqueous solution. There is a stationary region between the wall and the center, because the direction of fluid movement at the center part of the rectangular cell is opposite that of the wall side, and the electrophoretic mobility of bubbles at the stationary region can be correctly evaluated without the electroosmosis effect.[16] The previous works characterized the electroosmotic flow in the electrophoresis cell, and the bubbles in the region can be easily recognized by changing the direction of the electric potential drop alternately.[18] As shown in Figure 4, the trace line of the microbubble in the stationary region was clearly zigzagged with straight lines, while the movement of the bubble located in the electroosmotic area was disturbed by the inertial movement of the surrounding water and the trace lines were bent.

The ζ potential of bubbles in aqueous solutions was obtained using a graphic data processing method. Figure 5 shows the trace of bubble movement for about 3 s in the stationary region; the travel distance along the Y axis was related to the bubble size, and that along the X axis corresponded to electrophoretic mobility. The bubble diameter was obtained from the rising speed of the bubble according to the relationship shown in Figure 2; the data were obtained using the microscopic system with a higher magnification lens. The ζ potential was determined from electrophoretic mobility using the Smoluchowski equation as[19]

$$\zeta = \eta\mu/\epsilon$$

where ζ is the zeta potential (V), η is the viscosity of water (kg

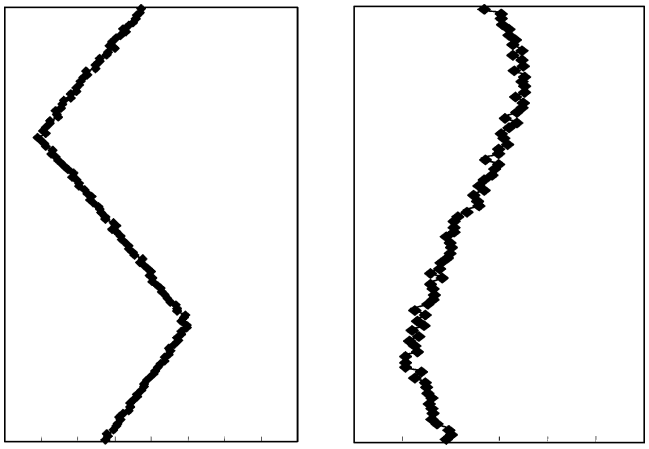

Figure 4. Examples of the shapes of bubble movement in the stationary level (left) and outside the level (right). The movement of the bubble located in the electroosmotic area was disturbed by the inertial movement of the surrounding water, and the trace lines were bent.

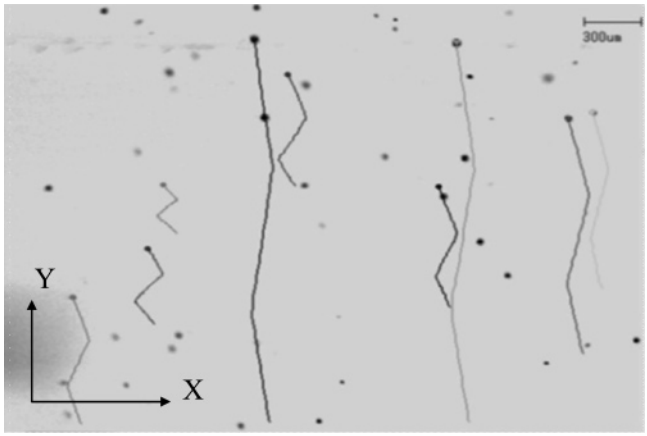

Figure 5. Traces of bubble movement for approximately 3 s. The ζ potential and the diameter of the microbubble were calculated from the velocity of the bubbles on *X* and *Y* axes, respectively. The alternative charge in the direction of the electrical potential drop made the bubbles turn in the cell. The bubbles affected by the electroosmotic flow were easily identified by the bubble movement because the inertial water movement in the electroosmotic area disturbed the quick turning of the bubbles.

m^{-1} s^{-1}), ϵ is the permittivity of water (kg^{-1} m^{-3} s^2 C^2), and μ is the mobility (m^2 s^{-1} V^{-1}).

ζ Potential of Microbubbles in Distilled Water

Most of the previous studies on the ζ potential of gas bubbles were conducted with water containing added electrolytes or surfactants, to generate small bubbles.[6−12,14,16] The ζ potential of the microbubble in distilled water is important as the basis of the gas−water interface charge, because the character of the gas−water interface charge in distilled water was simple due to the dilute ionic concentration. Figure 6 shows the ζ potential of microbubbles in distilled water. Despite no addition of electrolyte or surfactant, aside from dissolved ambient CO_2, the microbubbles were negatively charged with an averaged ζ potential of approximately −35 mV, in distilled water at pH 5.8. There was no relationship recognized between the magnitude of the potential and the bubble diameter.

Although the surface charge of colloidal material in water has been explained by the ionization of the surface of the material or the adsorption of an ionic surfactant, another charging mechanism must be considered for the gas−water

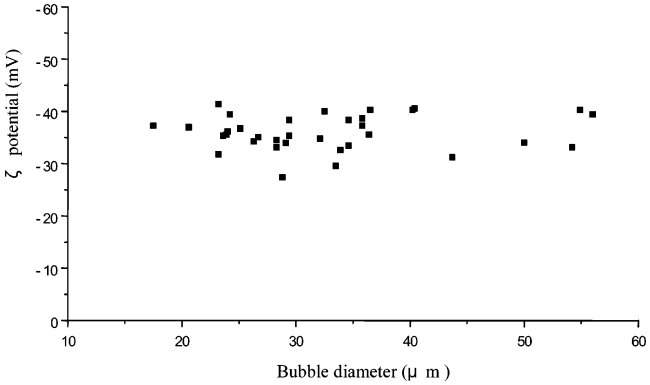

Figure 6. ζ potential of microbubbles in distilled water. Despite no addition of electrolyte or surfactant, aside from dissolved ambient CO_2, the gas−water interface was negatively charged and no appreciable variation in the potential was observed in correlation with bubble size.

interface, because the distilled water did not contain any ionic surfactant and the interior gas was not ionized in the normal condition of the experiment. The gas−water interface is negatively charged, so that OH^- must play an important role in the electrical charge. Experimental data obtained to date show that bubbles in water without any surfactant are negatively charged, and the charging mechanism has been explained by the excess of OH^- ions compared to H^+ ions at the gas−water interface. Most researchers have explained the adsorption of OH^- onto the interface by the difference of hydration energy between H^+ and OH^- or by the orientation of water dipoles at the interface, with hydrogen atoms pointing toward the water phase and oxygen atoms toward the gas phase, causing an attraction of anions to the interface.[7,9,10,14,16] To confirm these assumptions, more detailed data of the gas−water interface charge is required, and the charging mechanism will be discussed later.

The effect of bubble size on the ζ potential is of great interest, and the Dorn potential measurement by Usui et al. demonstrated that the variation in bubble surface charge depended on the bubble diameter.[20] However, in this study, there was no relationship recognized between the ζ potential of the microbubble and the bubble size, and the result suggested that the amount of electricity per unit surface area at the interface was not dependent on the bubble size. The extrapolation of the result of the microbubble to a bubble with infinite diameter suggested that the amount of electricity of a flat gas−water interface is the same as that of a microbubble.

Effect of an Inorganic Electrolyte on the ζ Potential

One predominant factor of the gas−water interface charge must be the role of ions at and near the interface. Most previous studies have recognized that the gas−water interface charge is caused by the adsorption of OH^- onto the interface, and some researchers have tried to explain the adsorption of the anion by the difference in the hydration energies of H^+ (−1127 kJ/mol) and OH^- (−489 kJ/mol).[7,9,10,19] In this section, the role of ions at and near the gas−water interface in the electrical charge is illustrated by the addition of electrolytes to distilled water.

If the hydration energy of an ion is a crucial factor of adsorption of the ion to the gas−water interface, it is of great interest to determine the effect of inorganic electrolytic ions, with a variety of hydration energies, on the electrical charge of the microbubbles. Figures 7 and 8 show the effect of NaCl and $MgCl_2$ on the ζ potential of the microbubbles, respectively. Both of the electrolytes caused a reduction in the ζ potential,

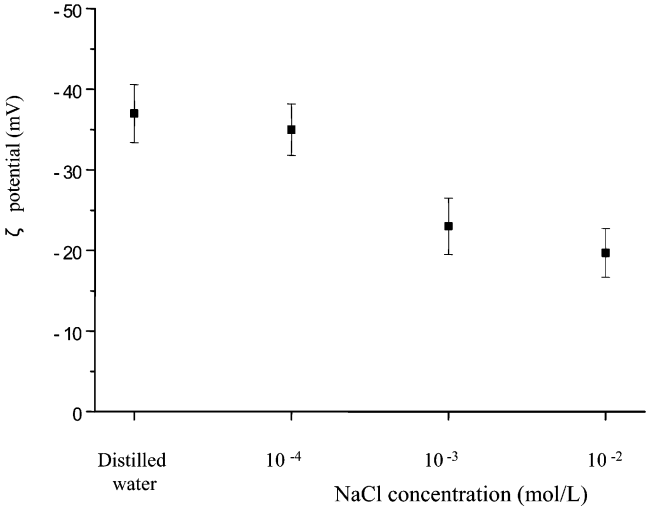

Figure 7. Relationship between the ζ potential of microbubbles and the concentration of NaCl in the water. The electrolyte reduced the ζ potential by increasing the amount of counterions within the slipping plane.

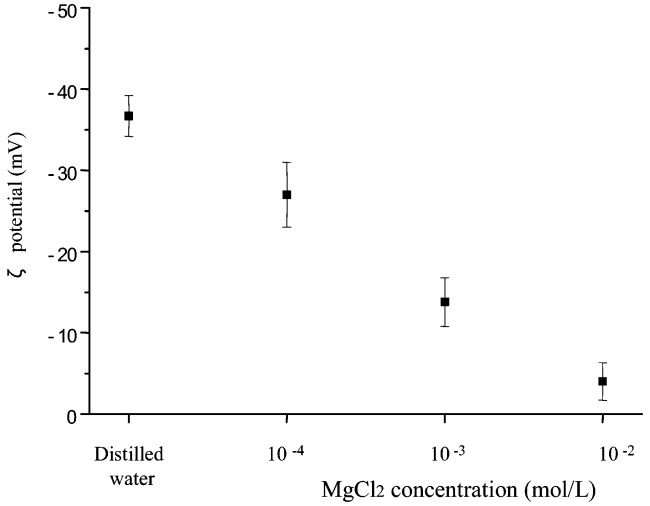

Figure 8. Relationship of the ζ potential of the microbubbles and the concentration of $MgCl_2$ in the water. The electrolyte reduced the ζ potential to a greater degree than NaCl, due to the difference in the ionic valency of the cations and the pH reduction of the water.

depending on their concentration. According to the assumption regarding the hydration energy, the Cl^- anion (−317 kJ/mol) tended to remain longer at the gas−water interface than the Na^+ cation (−406 kJ/mol) and Mg^{2+} (−1904 kJ/mol). It was expected that the negative value of the ζ potential of the microbubbles would increase; however, the results indicated the opposite effect of electrolytes on the ζ potential of the microbubble, especially in the case of $MgCl_2$, even though there is a bigger difference in the hydration energies of Mg^{2+} and Cl^- than the difference between H^+ and OH^-. It has been demonstrated that the difference in the hydration energies of inorganic electrolytes does not contribute to the adsorption of the ions for the gas−water interface charge.

Consideration of the reason for the strong reduction in the negative value of the ζ potential by the addition of $MgCl_2$ will contribute to a deeper understanding of the interface charge. The ionic valency of Mg^{2+} could be an important factor and will be discussed later in regard to the electric double layer. The interface electrical charge might be related to the amounts of H^+ and OH^- at the interface, because of the pH change of the aqueous solution according to the concentration of the electrolytes; this does not occur in the case of NaCl. Therefore, it would be very useful to clarify the effect of pH on the ζ potential of the microbubble.

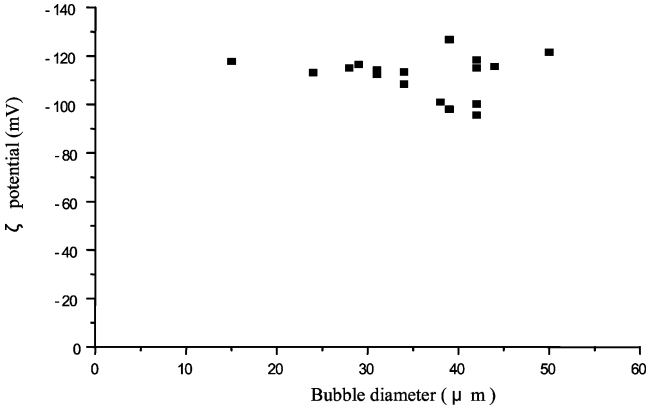

Figure 9. ζ potential of microbubbles at pH 10.26 determined by the addition of NaOH to distilled water.

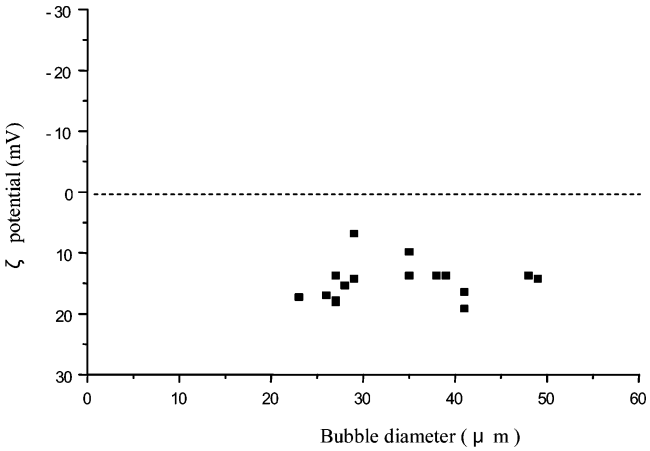

Figure 10. ζ potential of microbubbles at pH 2.68 determined by the addition of HCl to distilled water.

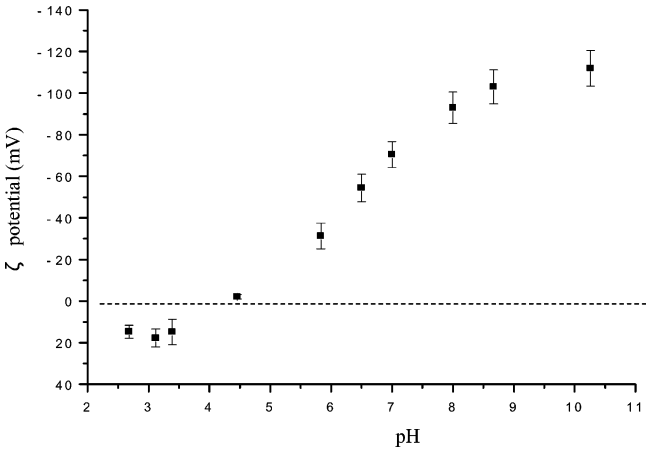

Figure 11. Relationship between the ζ potential of the microbubbles and the pH of the water, determined by HCl and NaOH. The surface charge of the gas−water interface was strongly affected by the pH of the water. The result indicated the important role of H^+ and OH^- in the surface charge.

Figures 9 and 10 show the ζ potential of microbubbles in water with pH 10.26 and 2.68. The value of the pH was adjusted by the addition of NaOH and HCl to distilled water at room temperature. Figure 11 shows the relationship between the average value of the ζ potential of the microbubbles and the pH of the water. The results demonstrated that there is a strong

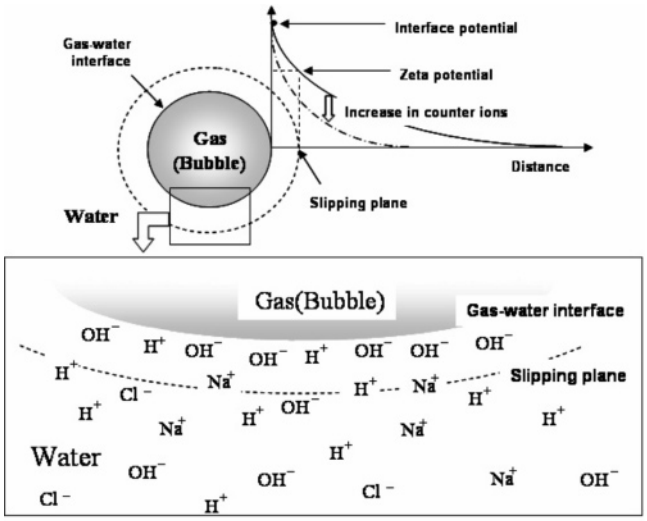

Figure 12. Distribution of ions at and near the gas−water interface in an aqueous solution of NaCl. The electrolyte ions are attracted to the interface charged by H^+ and OH^- and create the electrical double layer. The ζ potential is the electrical potential at the slipping plane, and the potential is determined by the amount of ions and their valency in the slipping plane.

effect of the pH of the water on the ζ potential of microbubbles. Under a wide range of pH conditions, the ζ potential indicated a negative sign and the negative value increased with increasing pH, until it reached a plateau of approximately −110 mV at pH ≈10. For acidic conditions below pH 4.5, the ζ potential of the microbubbles showed a positive value. The strong effect of pH on the ζ potential of the microbubbles indicated that both H^+ and OH^- played a very important role in the gas−water interface charge by adsorption of these ions at the interface and that other additional ions, such as Na^+ and Cl^-, did not have any significant effect on the ζ potential of the microbubble, besides their influence as counterions. The plateaus of the ζ potential at high and low pH were explained by H^+ and OH^- moving back to the bulk of water, due to the increased chemical potential at the interface. The fact that the interface is positively charged under strongly acidic conditions shows that there is an excess of H^+ over OH^- at the interface. It is difficult to explain the mechanism of the positively charged gas−water interface by the assumption of the orientation of water dipoles at the interface, as well as the difference of hydration energy between H^+ and OH^-, because both assumptions only explain the case for excess OH^- at the gas−water interface.

Figure 12 illustrates the distribution of ions at and near the gas−water interface in an aqueous solution of NaCl. The adsorbed H^+ and OH^- are crucial factors influencing the interface charge, and the electrolyte ions are attracted to the interface, as for the counterions, by electrostatic force and generation of the electrical double layer. The ζ potential is the electrical potential at the slipping plane, so that the increase in counterions reduces the ζ potential according to the number of counterions that exist between the interface and the slipping plane. As the force of the attraction depends on the valency of the counterions, ions with a valency of +2 or higher tend to be attracted to the interface more strongly than ions with a valency of +1, due to static electricity, and this results in a reduction of the ζ potential due to the dense concentration of the counterions inside the slipping plane.

The significant change in the ζ potential of the microbubbles, depending on the pH of the aqueous solution, suggests that H^+ and OH^- play an important role at the interface in the gas−water interface charge. The negative value of the ζ potential under the wide range of pH conditions suggests that OH^- tends to be more effectively adsorbed to the interface than H^+. The next investigation aims to clarify the mechanism of the adsorption of H^+ and OH^- to the gas−water interface.

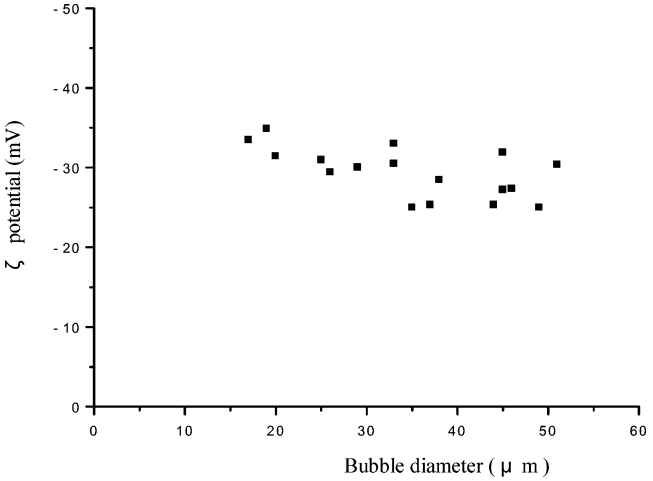

Figure 13. ζ potential of microbubbles in a binary mixture of 0.5% ethanol and water.

Effect of Additional Alcohol on the ζ Potential

It is demonstrated that H^+ and OH^- have an exclusive effect on the gas−water interface electrical charge. These ions are the essential elements of the hydrogen-bonding network of water, besides the H_2O molecule, so it is necessary to consider the charging mechanism from the point of view of the hydrogen-bonding network. The hydrogen-bonding network at the gas−water interface must be different from that in bulk water, because intermolecular cohesive forces in the interface phase are not compensated and the properties of a water interface layer, such as the density, viscosity, electrical conductivity, and dielectric permittivity, are different from those of the bulk water.[21] Investigations of molecular dynamics computer simulations and surface specific techniques, such as vibrational sum-frequency spectra, revealed an anomaly in the surface structure of water, such as the presence of the dangling OH stretch.[16,20,22−27] The purpose of this study is to illustrate the role of a hydration-bonding network in the gas−water interface electrical charge.

Some kinds of alcohols have a surface activity by being adsorbed to the gas−water interface, and the effect of disturbance of the hydrogen-bonding network at the interface on the electrical charge can be investigated by adding the alcohols to distilled water. Figures 13 and 14 show the ζ potential of the microbubbles in binary mixtures of ethanol−water and 1-propanol−water, respectively. In the case of 1-propanol, a wide spread of the ζ potential was observed with positively charged bubbles in the aqueous solution with pH 5.8, while the addition of ethanol did not disperse the ζ potential so widely. As shown in Figures 15 and 16, both alcohol additions resulted in reducing the negative value of the ζ potential of the microbubbles, depending on their concentration, and the significant difference between them was found in the distribution range of the ζ potential. It was also recognized that methanol had the same effect as ethanol on the ζ potential of the microbubble and that 2-propanol and butanol dispersed the ζ potential of the microbubble widely, as for 1-propanol.

The dilute binary mixtures of the lower primary alcohols, such as methanol−water and ethanol−water, have a similar network of hydrogen bonds with water, and the network is

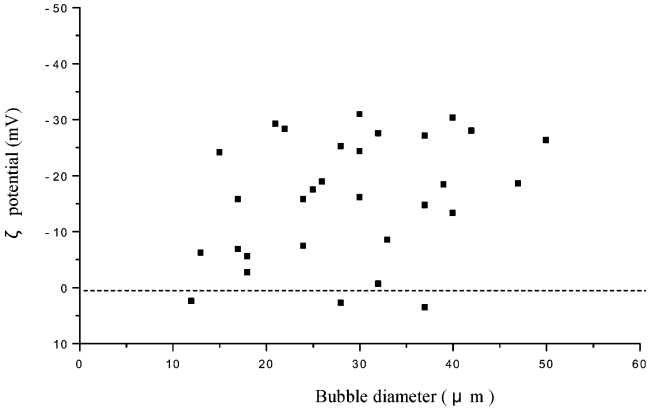

Figure 14. ζ potential of microbubbles in a binary mixture of 0.5% 1-propanol and water.

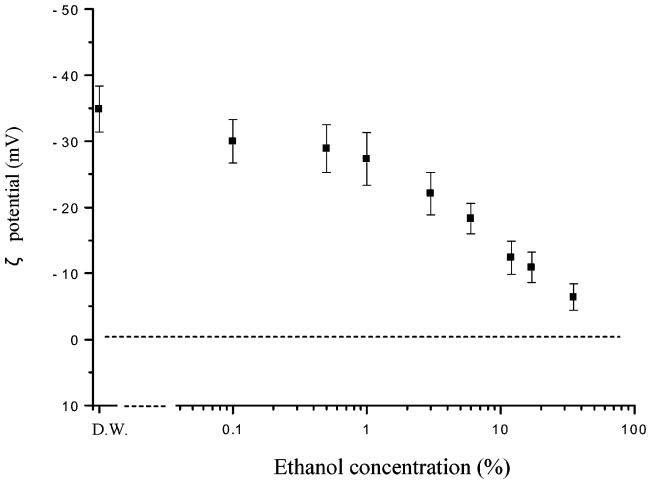

Figure 15. Relationship of the ζ potential of microbubbles and the concentration of ethanol mixed with water.

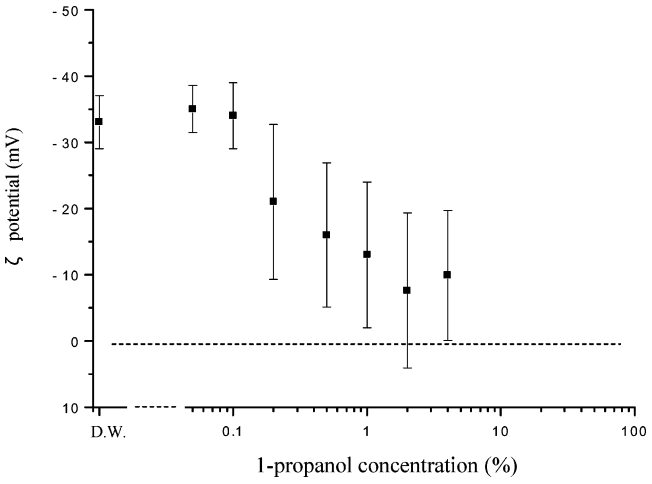

Figure 16. Relationship of the ζ potential of microbubbles and the concentration of 1-propanol mixed with water.

microscopically homogeneous throughout the bulk and the gas−water interface.[20,29,30] On the contrary, the mixtures of water and higher alcohols, such as propanol and butanol, have the same network structure of hydrogen-bonded linkage but are microscopically somewhat heterogeneous.[31−33] These alcohols tend to be adsorbed to the gas−water interface, so that the addition of a small amount of the alcohols significantly disturbed the hydrogen-boding network at the interface.

It has been demonstrated that the addition of salts to water−alcohol binary mixtures induces the separation of these molecules due to the increase in the microheterogeneity of the solution, as confirmed by liquid spray mass spectroscopy studies of their microscopic structure in aqueous solution.[34,35] Figure 17 shows the relationship between the average value of the microbubble ζ potential in 3% ethanol−water binary mixtures and the pH of the aqueous phase, adjusted by the addition of HCl and NaOH. The results indicate that, even when ethanol is used, the ζ potential values are widely dispersed following the addition of HCl and NaOH. Consequently, it may be assumed that the addition of HCl and NaOH causes the alcohol to adsorb to the gas−water interface due to the separation of water and the alcohol, resulting in the disturbance of the hydrogen-boundary network at the interface.

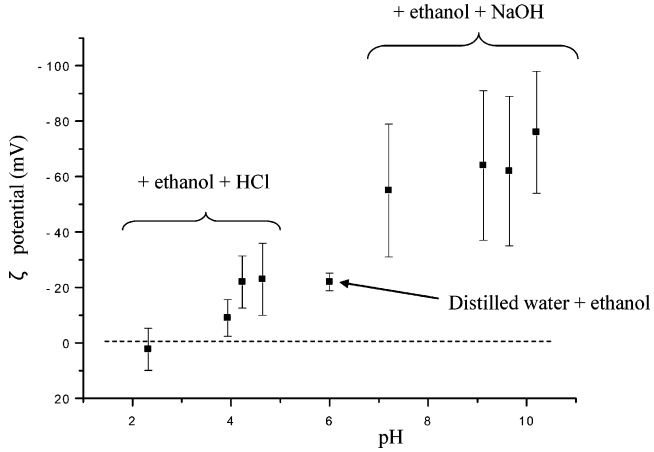

Figure 17. Relationship between the ζ potential of the microbubbles in 3% ethanol−water binary mixtures and the pH of the aqueous phase, adjusted by the addition of HCl and NaOH.

These alcohol molecules are not electrically charged, so the drastic change in the ζ potential of the microbubbles caused by the addition of these alcohols must be attributed to the change in the microscopic structure of the microbubble at the interface. These results demonstrate that the gas−water interface electrical charge is related to the hydrogen-bonding network of water. The electric charge of the interface in the aqueous solution is caused by a greater excess of H^+ and OH^- at the interface than in the bulk. These ions are the essential elements of the hydrogen-bonding network; therefore, the structural formation of the gas−water interface must include a greater number of these ions at the interface than in the bulk aqueous phase. As shown in Figures 11 and 17, the negative value of the ζ potential for the microbubble in a wide pH range suggests that OH^- is more effective than H^+ at influencing the microscopic structure of the gas−water interface.

Conclusion

Microbubbles are promising candidates for future practical applications, and they allow investigation of the electrical properties of the gas−water interface without the need for any complicated measuring methods. This study resulted in the clarification of the ζ potential of microbubbles in aqueous solutions and revealed that microbubbles are negatively charged under a wide range of pH conditions and positively charged under strongly acidic conditions. It was also demonstrated that OH^- and H^+ are crucial factors for the electrical charge of the gas−water interface and that the difference in the construction of the hydrogen-bonding network between the gas−water interface and the bulk of water must be attributed to an excess of these ions at the interface over the amount in the bulk.

Acknowledgment. This research was supported by grants from the Ministry of Education, Culture, Sports, Science and Technology and from National Institute of Advanced Industrial Science and Technology. The author also acknowledges Professor S. Mori, Dr. T. Furuyama of Kyushu University, and Dr. A. Wakisaka of National Institute of Advanced Industrial Science and Technology for their technical advice on conducting the research work and S. Taniguchi for assistance with data collection.

References and Notes

(1) Burns, S. E.; Yiacoumi, S.; Tsouris, C. *Sep. Purif. Technol.* **1997**, *11*, 221.
(2) Kodama, Y.; Kakugawa, A.; Takahashi, T.; Kawashima, H. *Int. J. Heat Fluid Flow* **2000**, *21*, 582.
(3) Takeuchi, S.; Sato, T.; Kawashima, N. *Colloids Surf., B* **2002**, *24*, 207.
(4) Takahashi, M.; Kawamura, T.; Yamamoto, Y.; Ohnari, H.; Himuro, S.; Shakutsui, H. *J. Phys. Chem. B* **2003**, *107*, 2171.
(5) Fukui, Y.; Yuu, S.; Ushiki, K. *Powder Technol.* **1988**, *54*, 165.
(6) McTaggart, H. A. *Philos. Mag.* **1922**, *44*, 386.
(7) Yoon, R.; Yordan, J. L. *J. Colloid Interface Sci.* **1986**, *113*, 430.
(8) Okada, K.; Akagi, Y.; Yoshioka, N. *Can. J. Chem. Eng.* **1988**, *66*, 276.
(9) Li, C.; Somasundaran, P. *J. Colloid Interface Sci.* **1991**, *146*, 215.
(10) Kim, J. Y.; Song, M. G.; Kim, J. D. *J. Colloid Interface Sci.* **2000**, *223*, 285.
(11) Collins, G. L.; Motarjemi, M.; Jameson, G. J. *J. Colloid Interface Sci.* **1978**, *63*, 69.
(12) Sherwood, J. D. *J. Fluid Mech.* **1986**, *162*, 129.
(13) Graciaa, A.; Morel, G.; Saulnier, P.; Lachaise, J.; Schechter, R. S. *J. Colloid Interface Sci.* **1995**, *172*, 131.
(14) Saulnier, P.; Lachaise, J.; Morel, G.; Graciaa, A. *J. Colloid Interface Sci.* **1996**, *182*, 395.
(15) Graciaa, A.; Creux, P.; Lachaise, J.; Salager, J. L. *Ind. Eng. Chem. Res.* **2000**, *39*, 2677.
(16) Yang, C.; Dabros, T.; Li, D.; Czarnecki, J. Masliyah, J. H. *J. Colloid Interface Sci.* **2001**, *243*, 128.
(17) Kelsall, G. H.; Tang, S.; Smith, A. L.; Yurdakul, S. *J. Chem. Soc., Faraday Trans.* **1996**, *92*, 3879.
(18) Phianmongkhol, A.; Varley, J. *J. Colloid Interface Sci.* **2003**, *260*, 332.
(19) Smoluchowski, M. *Z. Phys. Chem.* **1918**, *92*, 129.
(20) Usui, S.; Sasaki, H.; Matuskawa, H. *J. Colloid Interface Sci.* **1981**, *81*, 80.
(21) Paluch, M. *Adv. Colloid Interface Sci.* **2000**, *84*, 27.
(22) Matsumoto, M.; Kataoka, Y. *J. Chem. Phys.* **1988**, *88*, 3233.
(23) Benderskii, A.; Eisenthal, K. B. *J. Phys. Chem. B* **2000**, *104*, 11723.
(24) Yang, K. L.; Yiacoumi, S. *J. Chem. Phys.* **2002**, *117*, 337.
(25) Townsend, R. M.; Rice, S. A. *J. Chem. Phys.* **1991**, *94*, 2207.
(26) Scatena, L. F.; Brown, M. G.; Richmond, G. L. *Science* **2001**, *292*, 908.
(27) Raymond, E. A.; Tarbuck, T. L.; Richmond, G. L. *J. Phys. Chem. B* **2002**, *106*, 2817.
(28) Raymond, E. A.; Tarbuck, T. L.; Brown, M. G.; Richmond, G. L. *J. Phys. Chem. B* **2003**, *107*, 546.
(29) Wakisaka, A.; Usui, Y. *J. Mol. Liq.* **2001**, *90*, 175.
(30) Mashimo, S.; Kuwabara, S. *J. Chem. Phys.* **1989**, *90*, 3292.
(31) Chen, B.; Siepmann, J. I.; Klein, M. L. *J. Am. Chem. Soc.* **2002**, *124*, 12232.
(32) Vasquez, D.; Toro, J.; Lozsan, A.; Garcia-Sucre, M.; Urbina-Villalbe, G. *J. Phys. Chem. B* **2002**, *106*, 2649.
(33) Mashimo, S.; Umehara, T. *Chem. Phys.* **1991**, *95*, 6257.
(34) Wakisaka, A.; Mochizuki, S.; Kobara, H. *J. Solution Chem.* **2004**, *33*, 721.
(35) Wakisaka, A.; Ohki, T. *Faraday Discuss.* **2005**, *129*, 231.